Intracellular ionic concentration by calibration from fluorescence indicator emission spectra, its relationship to the K_d, F_{min}, F_{max} formula, and use with Na-Green for presynaptic sodium

James L. Winslow [a,b,*], Robin L. Cooper [a,c], Harold L. Atwood [a]

[a] Physiology Department, University of Toronto, Toronto, ON, Canada M5S 1A8
[b] Institute of Biomaterials and Biomedical Engineering, University of Toronto, Toronto, ON, Canada M5S 1A8
[c] Thomas Hunt School of Biology, University of Kentucky, Lexington, KY 40506-0225, USA

Abstract

The emission spectra calibration curves for a fluorescence indicator and the F_{min}, F_{max}, and K_d formula were shown to be related. Using the known calibrated fluorescence emitted by Sodium Green (Na-Green) and photo-multiplier-tube quantum efficiency, we calculated the detection signal over a range of sodium concentrations. The calculated calibration curves were compared for optical filters passing a narrow band, medium band or full spectrum. We found that a method based on the full emission spectrum was the most appropriate. Given a known resting concentration of intracellular sodium, calibrated readings can be converted to concentration values. This method is applicable to any fluorescence indicator when curves for emission spectra over a range of concentrations are available. We measured sodium concentration changes during trains of action potentials (APs) at a crayfish motor axon's presynaptic terminals injected with Na-Green. During low frequency AP trains, net sodium increases asymptotically with frequency. Average net Na-flux per AP decreases for increasing terminal size. The terminals of crayfish motor axon have surface area to volume ratio which is 7700 times larger than for squid. Thus, in comparison to squid, crayfish terminals exhibit a larger change in $[Na^+]_i$ during equivalent AP activity. © 2002 Elsevier Science B.V. All rights reserved.

Keywords: Area ratio method; Channel density; Ratiometric formula; Area to volume ratio; Sodium flux density; Fluorescence calibration

1. Introduction

Fluorescent dyes are routinely used with confocal microscopy to determine intracellular concentration of ions during physiological experiments. Changes in ionic concentrations activate or control mechanisms, hence measurement precision is an issue. We investigated a procedure for estimating ionic concentration with a non-ratiometric indicator dye.

There are two methods to determine concentration using fluorescence light. In the case of dyes (e.g. the Na^+-sensitive indicator SBF1) for which the absorbed fluorescence spectrum is altered by concentration change, the emitted fluorescence can be measured at two different wavelengths and the ratiometric method (RMM) used to determine concentration changes (Grynkiewicz et al., 1985; Harootunian et al., 1989; Minta and Tsien, 1989; Tsien and Waggoner, 1995). In contrast, for a monochromatic or near-monochromatic dye such as Sodium Green (Na-Green) (Molecular Probes Handbook, 1998; Szmacinski and Lakowicz, 1997) the ratio of fluorescence change to resting fluorescence is measured within a filtered interval of light wavelengths. Usually, only relative concentration change is given (Regehr, 1997). Near-monochromatic dyes are widely used and many papers in the literature report relative fluorescence change; if this was converted to concentration units, comparisons with other data would be possible.

If fluorescence intensity were linearly related to concentration, the relative ionic concentration could be estimated. However, the relationship is not linear over a wide concentration range. We analyzed the

* Corresponding author. Tel.: +1-416-978-2680; fax: +1-416-978-4940

E-mail address: winslow@spine.med.utoronto.ca (J.L. Winslow).

calibration curves and derived an *area ratio method* (ARM) in which the ensemble of intensities at all wavelengths (λ) of emitted fluorescence is used as the detection signal. Since light intensity data are collected for $a \leq \lambda < \infty$, where a is the lower cutoff wavelength of the filter, the calculated calibration curve has to reflect this. It will be shown that: (1) narrow band optical filters are not as accurate because they omit data, particularly when normalization is used; (2) the ARM calibration curve, which does not require measurement of maximum fluorescence (F_{max}) is related to the equation that uses F_{min}, F_{max}, and K_d, where F_{min} is minimum fluorescence and K_d is the dye dissociation constant; and (3) when resting concentration is available, the absolute concentration change can be calculated; and (4) this method is applicable to any fluorescent indicator when the emission spectra versus concentration curves are available.

We employed the ARM to estimate sodium concentration in crayfish presynaptic terminals during low frequency (≤ 15 Hz) stimulus pulse trains. We found that presynaptic sodium concentration increases twofold during AP trains at relatively low frequencies in relatively small nerve terminals of crayfish neuromuscular junctions. These terminals have a larger surface area to volume ratio than squid giant synapse, in which a small increase was reported for comparable stimulus frequencies (Hodgkin and Keynes, 1955). The ARM enhances the opportunities for experimental comparison of Na^+ dynamics in different nerve terminals. A preliminary report of this work appeared in abstract form (Winslow et al., 1996).

2. Methods and materials

We used Na-Green, impermeant form (Molecular Probes, Inc. S-6900, lot #2241, $K_d = 21.0$ mM), as the fluorescence indicator for Na^+ in conjunction with confocal microscopy to measure the sodium response to stimulation at the crayfish opener neuromuscular preparation. See Figs. 1A and 3.

2.1. Measured fluorescence ratio

The relative emitted fluorescence light from a source region is,

$$\bar{F} = (F_{stim} - F_{rest})/F_{rest},$$

where F_{stim} and F_{rest} are the fluorescence intensities measured during stimulation and rest, respectively. F_{rest} reflects the intra-terminal value, and confocal microscopy helps to remove the effects of tissue absorbance. A larger varicosity may appear brighter than a small varicosity because fluorescence at a single image pixel $F(x, y)$ is the result of summing the signal along the z-

column perpendicular to the plane of the image and interior to the region.

Total fluorescence from the region is the sum of the $F(x, y)$ values in the region. If $f(p)$ is fluorescence per voxel at (x, y, z), then the total detected fluorescence for region R with volume V is,

$$F(R) = \int_R f(p)\, dv,$$

where dv is an element of volume, i.e. voxel. Thus average fluorescence in the region is,

$$\hat{F}(R) = \frac{1}{V} \int_R f(p)\, dv.$$

The rest and stimulated average values are, respectively $\hat{F}_{rest}(R) = F_{rest}(R)/V$ and $\hat{F}_{stim}(R) = F_{rest}(R)/V$. Replacing F_{stim} and F_{rest} by $\hat{F}_{stim}$ and $\hat{F}_{rest}$ in the formula for $\bar{F}$ gives,

$$\hat{\bar{F}}(R) = (\hat{F}_{stim}(R) - \hat{F}_{rest}(R))/\hat{F}_{rest}(R)$$
$$= (F_{stim}(R) - F_{rest}(R))/F_{rest}(R),$$

hence, $\hat{\bar{F}}(R) = \bar{F}(R)$. Thus $\bar{F}(R)$ is the normalized average fluorescence over the measured region. Consequently, since V does not appear in the equation for $\bar{F}(R)$, size of the terminal does not influence the $\bar{F}(R)$ measurements. Fig. 3 shows $\bar{F}$ in relative fluorescence units for the wavelength pass interval $[a, b) = [515, \infty)$ nm. Note that, square brackets denote end point membership in the interval, whereas parentheses do not.

2.2. Detection signal

The calibration curves for Na-Green (Molecular Probes Handbook, 1998, Fig. 24.5, bottom) were measured from lot #2241 and #2231, which, respectively displayed a $7.8 \times$ and $7.0 \times$ increase in emission intensity at maximum compared with background (difference due to path absorbance). When normalized to the maximums, the curves were identical. The purity of both lots was 96% by HPLC; the extinction coefficient for lot 2241 was 157 357 and for lot 2231 was 158 300/cm/M. For all lots, 200 nM NaCl in 10 mM MOPS (pH 7.2) was used (Molecular Probes technical discussion).

The calibration curves give relative fluorescence versus emitted light wavelength $F(\lambda, Na)$ for different concentrations of sodium, $Na \equiv [Na^+]$ (to abbreviate). The emitted light after passing through filter(s) of net pass interval $[a, b]$ is detected by a photo-multiplier-tube (PMT) with quantum-efficiency response curve $E(\lambda)$ (BioRad MRC-600 Handbook) which is the relative efficiency of capturing photons of wavelength λ. Consequently, the resultant fluorescence signal $s(Na)$ measured per Na value is,

$$s(\text{Na}) = \int_a^b F(\lambda, \text{ Na}) \, E(\lambda) \, d\lambda.$$

To calculate $s(\text{Na})$, we need $F(\lambda, \text{ Na})$ and $E(\lambda)$. See Fig. 1B.

Note that the quantum-efficiency response curve $E(\lambda)$ varies across PMTs. Thus the $E(\lambda)$ curve specific for the detection system used, is required. See Section 4.

2.3. Area ratio method

The essential concept of the ARM is to calculate the ratio of areas under the emission spectra curves (N_c of them) which change for different concentrations of the target ion. Specifically the ARM uses: (1) the full pass spectrum of emitted light $a \leq \lambda \leq b$; (2) the calibrated emission response of the indicator dye; (3) rescaling to remove attenuation of the signal by intervening tissue; (4) the calibrated efficiency of the PMT; and (5) rescaling to remove gain of the electronics. Because calibrated intermediate signals are used, concentration values are available when a reference concentration is available.

2.4. ARM steps

The steps in the conversion of the emitted fluorescence F to calibrated signal, $S(\text{Na})$ are shown in Fig. 1. The calibrated total emitted fluorescence, $S(\text{Na})$ versus Na is equivalent to the area under each curve for $E(\lambda)F(\lambda, \text{ Na})$, normalized to the area under the curve for $\text{Na} = 0$, as shown in Fig. 1D.

For $F(\lambda, \text{ Na})$, the calibration curves (Molecular Probes Handbook, 1998) for Na-Green with $[\text{Na}^+]_i + [\text{K}^+]_i = 135$ mM were digitized as one image. The axes and curves were each traced as a polygonal line (Winslow et al., 1987) and stored in an ASCII file of (X, Y) pixel coordinates. A program written by JLW read and processed data from this file. The sequence of points for each polygonal line per Na value was translated and rotated such that the abscissa was horizontal and the origin was at $(0, 0)$, then scaled appropriately. The resultant points,

$$\{(\lambda_i, F_i); \; i = 1, 2, \ldots, N_j\},$$

give values for $F(\lambda, \text{Na}_j)$ versus λ curve, for the different Na_j; $j = 1, 2, \ldots, N_c$. N_j varied, $80 \leq N_j \leq 120$, depending on the curvature of the graphs. A cubic spline function (Johnson and Riess, 1977; Press et al., 1988) was fit to each $F(\lambda, \text{Na})$ versus λ curve. Each curve was interpolated using the fitted cubic spline interpolation, then expressed as $F(\lambda, \text{Na})/\max F_0$ where $\max F_0$ is the maximum of $F(\lambda, \text{Na})$ versus λ for $\text{Na} = 0$ as shown in Fig. 1A.

The figure of the curve for the PMT provided for the BioRad MRC-600 was similarly converted to a digital function for $E(\lambda)$, and expressed as a ratio, $0 \leq E(\lambda) \leq 1$, with respect to the peak; see Fig. 1B. Fig. 1C shows the result of the product of cubic spline interpolant functions $F(\lambda, \text{Na})E(\lambda)$. The value of $s(\text{Na})$ per Na value was computed using the product of the cubic spline functions for F and E then integrated by the trapezoid rule (Johnson and Riess, 1977; Press et al., 1988). Next, the normalized fluorescence signal,

$$S(\text{Na}) = s(\text{Na})/s(0),$$

versus Na ($S(0) = 1$) was calculated and is shown in Fig. 1D, middle curve($+$), for each of the N_c concentrations in Fig. 1A.

2.5. Interpolation

The digitized points of the $F(\lambda, \text{Na}_j)$ versus λ curves, were linearly interpolated by using the trapezoid rule for integration. To evaluate $S(\text{Na})$ between the data points $S(\text{Na}_j)$ versus Na_j; $j = 1, 2, \ldots, N_c$ we can use linear interpolation or a cubic spline. Linear interpolation is shown by the dashed line in Fig. 1D. The cubic spline method of interpolation gives continuous first and second derivatives at the data points (knots of the cubic spline) and is preferable because it yields a smooth curve. A cubic spline function was calculated for these data points as shown by the solid middle line in Fig. 1D. See Section 4.

2.6. Calibration

Two reference points are available in the experimental data, namely, $S(\text{Na})$ for $\text{Na} = 0$ and $\text{Na}^r = [\text{Na}^+]_i^0 = 17.4 \pm 0.4$ mM, the resting value in crayfish axon (Wallin, 1967; Atwood, 1982). We use Na^r, from ventral cord axon in the same species *Procambarus clarkii*, and assume that Na^r is the same as in motoneurons and corresponds to F_{rest} in the measurements. The calibrated value Na^r (Wallin, 1967) has small standard error because large cytoplasm samples were taken from a large axon and integrating flame photometry was used to determine concentration. The appropriate calibrated response is,

$$\Phi(\text{Na}) = (S(\text{Na}) - S(\text{Na}^r))/S(\text{Na}^r)$$
$$= (s(\text{Na}) - s(\text{Na}^r))/s(\text{Na}^r).$$

The raw fluorescence signal from a region (reg) measured in an experiment, $F_{\text{stim}}(\text{reg})$, corresponds to the signal $s(\text{Na})$ and $F_{\text{rest}}(\text{reg})$ corresponds to the calibration signal in the region.

$$s(\text{Na}^r) = \int_a^b F(\lambda, \text{ Na}^r) \, E(\lambda) \, d\lambda.$$

Thus, the normalized fluorescence signal, $\bar{F}$, will equal the calculated calibration response Φ(Na). Hence, the sodium concentration is given by the inverse function for Φ.

$$\text{Na} = \Phi^{-1}(\bar{F}),$$

which is calculated by linear interpolation from the (Na, Φ) data points. The curve for Φ(Na) is shown in Fig. 2 as the dark center curve. There were 135 data

points, originating from the integer values of λ in $[a, b]$, where $F(\lambda, \text{Na})E(\lambda)$ is non-zero.

2.7. Relation to equation using F_{min}, F_{max}, and K_d

Because fluorescence emitted by dyes such as Na-Green or calcium green-5N do not show shifts in excitation or emission spectra on binding their targeted ions, it is not possible to use ratiometric measurements to calibrate fluorescence in terms of absolute free ionic
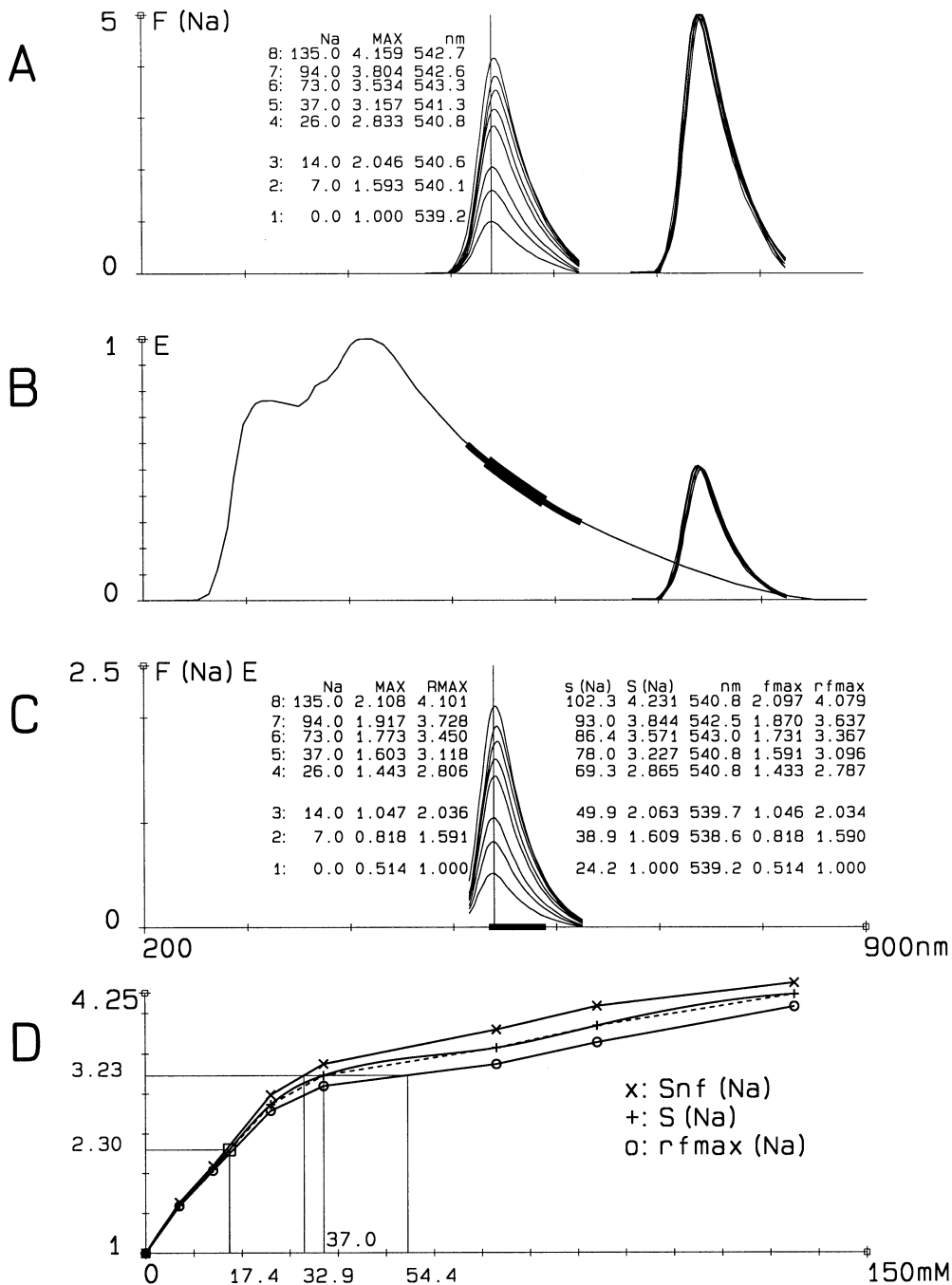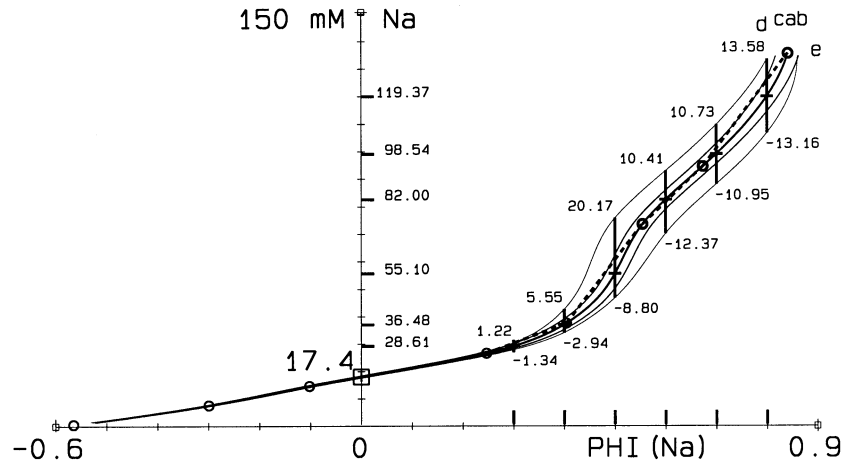

Fig. 1

Fig. 2. Comparison of calibration curves for area ARM with different wavelength pass intervals. Circles: ARM calculated data points $S(Na_j)$ versus Na_j, shown in Fig. 1D, now plotted as Na_j versus $\Phi(Na_j) = (S(Na_j) - S(Na^r))/S(Na^r)$; $j = 1, 2, \ldots, N_c$. The dashed lines are the linear interpolant between these points and the smooth curve (a) is a cubic spline fitted to these data points. Since $\bar{F} = \Phi(Na)$, thus $Na = \Phi^{-1}(\bar{F})$. For the assumed resting concentration of sodium, $Na^r = 17.4 \pm 0.4$ mM in crayfish axons, three curves (b, a, c) for Na versus $\Phi(Na)$ are calculated, respectively using $Na^r = 17.0, 17.4, 17.8$ mM. IRM (d): Data points which are the normalized values of $F(Na)E$ at λ_0, i.e. Na versus rfmax(Na). ARM (e): Same as ARM but with a band filter $[\lambda_0 - 5, \lambda_0 + 50]$ nm (heavy bold interval on horizontal axes of Fig. 1C). For $\bar{F} = \Phi(Na)$ values (thick horizontal axis marks) the corresponding $Na = \Phi^{-1}(\bar{F})$ values are shown (thick vertical axis marks). The thick vertical marks on the curve show the difference in mM between $rfmax^{-1}(\bar{F})$ (d) and ARM (a) and between $Snf(\bar{F})$ (e) and ARM (a). Scales: horizontal: $[-0.6, 0.9]$ dimensionless, vertical: $[0, 150]$ mM. See text.

concentration. Consequently, ionic concentration [ion] can be related to fluorescence (F), F_{min}, and F_{max} using the dissociation constant (K_d) by the equation,

$$[\text{ion}] = K_d \frac{(f - f')}{(1 - f)} = K_d \frac{(F - F_{min})}{(F_{max} - F)},$$

where F_{min} and F_{max} are the minimum and maximum possible fluorescence, $f = F/F_{max}$ and $f' = F_{min}/F_{max}$ (Tucker and Fettiplace, 1995; Grynkiewicz et al., 1985). The calibration function $S(Na)$ calculated from

$F(Na, \lambda)$, $E(\lambda)$, and F_{min}, can be related to a corresponding equation using F_{min} and F_{max} as follows.

Following Grynkiewicz et al. (1985), we assume that dye concentration and path length are small enough for the fluorescence contribution from any given molecular species to be proportional to the concentration of that species measured at wavelength λ. The proportionality constants are A_f for free dye and A_b for bound dye. For a mixture of free and ion-bound indicator at respective concentrations C_f and C_b, the total fluorescence intensity at wavelength λ will be given by,

Fig. 1. Steps in calculated calibrated emitted fluorescence, $S(Na)$. (A) Digitized fluorescence versus emitted light wavelength and sodium concentration curves. To simplify notation, let $Na = [Na^+]$. The calibration curves for Na-Green (Molecular Probes Handbook, 1998, Fig. 24.5, bottom) were digitized as an image. Each of the $N_c = 8$ curves was traced as a polygonal line which gave fluorescence $F(\lambda, Na)$ for emitted wavelength λ nm and sodium concentration Na_j mM, $j = 1, 2, \ldots, N_c$. A vertical line is drawn at $\lambda_0 = 539.2$ nm where $F(Na)$ is maximum for $Na = 0$ mM. Note that the maxima per curve do not occur at the same wavelength. See text. Inset text: Values per curve of Na, maximum and corresponding wavelength, λ. Inset figure on right: Each of the curves is shown normalized to full scale and shifted to the right by 200 nm (for inset) to show variation in shapes. (B) Efficiency of PMT versus wavelength. Plot of traced polygons from the digitized image of attenuation of the confocal microscope PMT (BioRad MRC-600). Shown on the curve is the interval of wavelengths for which the Na-Green calibration are computed $[a, b] = [515, 625]$ nm (bold) and through the narrow band filter $[\lambda_0 - 5, \lambda_0 + 50]$ nm (heavy bold). Horizontal axis as in A. Vertical axis is scaled to $[0, 1]$ as the curve is for relative efficiency. Inset figure on right: Each of the normalized curves in A has been multiplied by $E(\lambda)$ and shown with respect to full scale for comparison with A. (C) Product of emitted fluorescence and PMT efficiency, $E(\lambda)F(\lambda, Na)$ versus λ. The vertical line is at λ_0 as in A. Note that the maxima per curve does not occur at the same wavelength. This wavelength is coincidently the same in panels A and C for the bottom curves, but for all the other curves the maxima in A and C are shifted. Shown in bold on the horizontal axis is the interval for the narrow light filter $[\lambda_0 - 5, \lambda_0 + 50]$ nm. Inset table gives values per emission spectra curve: Na, MAX = maximum, RMAX = ratio of maximum, $s(Na)$ = area, $S(Na) = s(Na)/s(0)$, nm = λ_0 wavelength at maximum, fmax = value at λ_0, rfmax = ratio of value at λ_0. Due to the long pass light filter at 515 nm, the interval of integration is $[a, b]$, hence the clipped lower left ends of the curves. (D) Comparison of calibrated total emitted fluorescence, $S(Na)$, versus sodium concentration Na, with ratios of fluorescence, rfmax(Na), and Snf(Na). Each data point of $S(Na)$ is the area under each $F(Na)E$ curve in C which is normalized to the area under the curve for $Na = 0$. Thus $S(Na_j) = s(Na_j)/s(0)$, $j = 1, 2, \ldots, N_c = 8$. These data points (+) are linearly interpolated (dashed line) and fitted by a cubic spline polynomial (solid line). Each data point (o) of rfmax(Na) is computed from each $F(Na)E$ curve by taking the ratio of $F(Na)E$ evaluated at λ_0 over the value for λ_0, then fitted by straight line segments. The data points (x) for Snf(Na) are the same as $S(Na)$ but are only integrated over $[\lambda_0 - 5, \lambda_0 + 50]$ nm to demonstrate the effect of using a narrow filter. Shown by a box and thin line is the resting concentration of Na^+ in crayfish axon (Wallin, 1967) and its corresponding emitted fluorescence. For a relative fluorescence value of 3.23 the corresponding Na^+ concentrations are 32.9, 37.0, 54.4 from the Snf, S, and rfmax curves, respectively.

$$F = A_f C_f + A_b C_b.$$

At equilibrium C_f and C_b are related to $Na \equiv [Na^+]$ by the effective dissociation constant, $K_d = Na C_f / C_b$, thus

$$F = (A_f + A_b Na/K_d) C_f.$$

The total indicator is $C_{tot} = C_f + C_b = (1 + Na/K_d) C_f$. Solving for C_f gives,

$$C_f = \frac{C_{tot} K_d}{K_d + Na},$$

and

$$F = \frac{(A_f K_d + A_b Na) C_{tot}}{K_d + Na}.$$

If there is no free indicator, then $C_{tot} = C_b$ and $F_{max} = \mathrm{limit}_{Na \uparrow \infty} F = C_{tot} A_b$. If there is no bound indicator, then $C_{tot} = C_f$ and $F_{min} = \mathrm{limit}_{Na \downarrow 0} F = C_{tot} A_f$. Thus

$$F = \frac{F_{min} K_d + F_{max} Na}{K_d + Na}, \tag{1}$$

and solving for concentration Na gives,

$$Na = K_d \frac{F - F_{min}}{F_{max} - F}. \tag{2}$$

The calculated signal $s(Na)$ corresponds to the measured fluorescence F and $s(0) = F_{min}$, thus

$$\bar{F} = \frac{F - F_{min}}{F_{min}} = \frac{s(Na) - s(0)}{s(0)} = S(Na) - 1. \tag{3}$$

Since F_{max} is the limit of F when Na goes to ∞, we have $F_{min} \leq F < F_{max}$ and thus,

$$0 \leq \bar{F} < (F_{max} - F_{min})/F_{min}. \tag{4}$$

Substituting the above expression (1) for F into the definition (3) of $\bar{F}$ gives,

$$\bar{F} = \frac{(F_{max} - F_{min}) Na}{(K_d + Na) F_{min}}. \tag{5}$$

Note that if concentration $Na \downarrow 0$, then $F = F_{min}$, $\bar{F} = 0$, and $S(Na) = 1$. Solving for F_{max} gives,

$$F_{max} = (\bar{F}(K_d/Na + 1) + 1) F_{min},$$

and taking the limit of both sides as Na increases to infinity,

$$F_{max} = \left(\lim_{Na \uparrow \infty} \bar{F} + 1 \right) F_{min},$$

thus

$$\lim_{Na \uparrow \infty} \bar{F} = \frac{F_{max} - F_{min}}{F_{min}}, \tag{6}$$

which agrees with the inequality (4). Because $\bar{F} = S(Na) - 1$, we have

$$\lim_{Na \uparrow \infty} S(Na) = F_{max}/F_{min}. \tag{7}$$

Thus from Eqs. (3) and (5),

$$\bar{F} + 1 = S(Na) = \frac{(F_{max} - F_{min}) Na}{(K_d + Na) F_{min}} + 1. \tag{8}$$

Since F_{min} is defined to be the fluorescence when there is no Na^+ bound to the indicator, thus $s(0) = F_{min}$. Thus $S(Na)$ in Fig. 1D can be visually inspected for F_{max}/F_{min} or using the equation with $x = Na$, $y = S(Na)$,

$$y = 1 + \frac{ax}{b + x},$$

where the coefficients a and b are found by a best fit to the curve. Then $F_{max}/F_{min} = 1 + a$ and $K_d = b$, where $F_{min} = s(0)$. Recall that rectangular hyperbola $y = ax/(b+x)$ is the form of the Michaelis–Menten equation in enzyme kinetics (Horton et al., 1996).

We have demonstrated a one-to-one correspondence between points of $S(Na)$ versus Na and points of $\bar{F}(Na)$ versus Na which is continuous.

2.8. Demonstration preparation

The presynaptic motor nerve terminals at the crayfish opener neuromuscular preparation (Wojtowicz and Atwood, 1985) were prepared as previously described (Cooper et al., 1996). We used Na-Green, impermeant form (Molecular Probes, Inc. S-6900) as the fluorescence indicator for Na^+ with confocal microscopy to measure the response to stimulation by a current pulse train of increasing steps in frequency, at 20 °C.

The tip of the injection electrode was backfilled with a solution of 3 μM Na-Green dissolved in 50 mM KCl. The indicator was loaded into the crayfish exciter opener motor axon by pressure injection (range 20–60 psi). After the axon and its varicosities were visible, the injections were stopped and the axon varicosities were imaged with the BioRad MRC-600 laser confocal microscope (40× Nikon, water immersion lens, 488 nm excitation wavelength). The nerve was stimulated while recording the fluorescence signal without saturation of the dye. The emitted fluorescence of Na-Green in response to $[Na^+]_i$ passed through a filter with a wavelength pass interval $[a, b] = [515, \infty)$ nm, then detected by a PMT at 1 frame/s, and averaged over the stimulus-record interval. In the digitized confocal video images, the varicosities were outlined and the change in fluorescence measured (see Fig. 3).

3. Results

The calibration of the ARM is dependent on the wavelength pass interval $[a, b]$ and hence the limits of integration. We evaluated the affect of the interval size on accuracy and found that the widest interval gave the
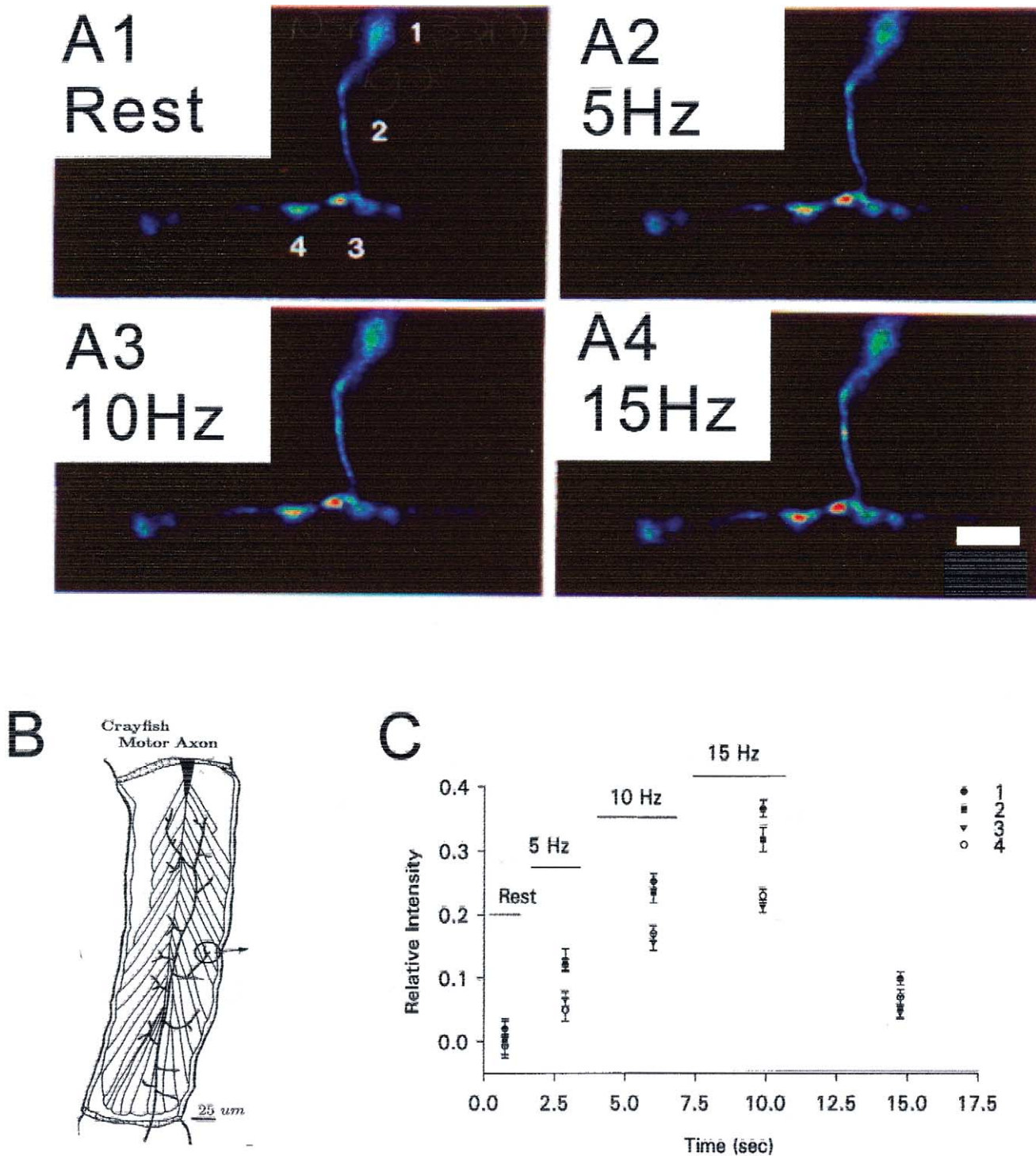
Fig. 3. Response of Na-Green fluorescence in nerve terminal. (A) Axon, showing recording regions and responses. (1) Rest, 1.00 s; (2) 5 Hz, 1.75 s; (3) 10 Hz, 3.75 s; (4) 15 Hz, 3.25 s. Not shown 0 Hz for 5.00 s. Scale bar (4): 20 μm. (B) Recording region of crayfish excitatory motor axon innervating the opener muscle. The circle indicates the recording region, where panel A is the circle in panel B rotated 30° counter-clockwise. (C) Relative intensity of Na-Green at the stimulus frequencies measured over the pixels in the lighted regions. The fluorescence signal $\bar{F}$ for the pixels within each recording region (reg) was averaged over the duration times at each given frequency. $\bar{F} = (F_{stim} - F_{rest})/F_{rest}$, where F_{stim} and F_{rest} are the measured fluorescence during stimulation and initial rest (0 Hz), for each region.

best results. Na-Green signals from presynaptic axonal varicosities were then used to demonstrate the ARM. The test demonstrated that relative fluorescence and hence $[Na^+]_i$ increases with stimulus frequency.

3.1. Effects of varying filter interval width

We compared the ARM using a long pass filter and hence integration over $[a, b) = [515, \infty)$ nm, with: (1) a worst-case use of the wavelength pass interval when $a = b$, denoted as the intensity ratio method (IRM), i.e. a filter passing only one wavelength is between the tissue and the PMT; (2) the case in which a narrow band filter $\lambda_0 \pm 10$ nm is used, for wavelength λ_0, where $F(\lambda, Na)$ is maximum for $Na = 0$; and (3) the case in which a narrow band filter $[\lambda_0 - 5, \lambda_0 + 50]$ nm is used as reported by some investigators. Thus we demonstrate the affects of varying the width of the filter interval.

3.1.1. IRM: Single wavelength filter

The maximum of each $F(\lambda, Na)E(\lambda)$ was calculated and normalized with respect to the curve for $Na = 0$ (MAX and RMAX in the inset table of Fig. 1C), then plotted as rfmax(Na) in Fig. 1D (lower curve). Note in Fig. 1C, that the wavelength, λ, at which $F(Na)$ and $F(\lambda, Na)E(\lambda)$ is maximum, per Na value, is not constant.

3.1.2. Narrow band filter

When a filter $[\lambda_0 - 10, \lambda_0 + 10]$ nm is used (data not show), the resulting calibration curve is almost exactly the same as the result for the single wavelength, except for a slight (1% difference) in the two largest Na calibration values.

3.1.3. Band filter

When a filter interval $[\lambda_0 - 5, \lambda_0 + 50]$ nm (thick bar on horizontal axis of Fig. 1C is used), the resulting calibration curve, Snf(Na) is greater than the result for the ARM approach, $S(Na)$, as shown in Fig. 1D (upper curve). For the unnormalized signals, $Snf(Na) \leq S(Na)$ because there is less area under the $F(Na, \lambda)E(\lambda)$ curves when integrated. However, when normalized $S(Na) \leq Snf(Na)$. In Fig. 1D, the difference in the Snf(Na), $S(Na)$, and rfmax(Na) curves increases for $Na > 25$ mM because the area under the curves is non-linear with respect to the maximum of the curves. For a relative fluorescence value 3.23 on the vertical axis, the corresponding value of Na on the horizontal axis using Snf(Na) is 32.9 mM; using $S(Na)$ the Na value is 37.0 mM, and using rfmax(Na) the Na value is 54.4 mM (by linear interpolation).

3.2. Calibrated concentration

A cubic spline function was fitted to the calibrated response of Na versus Na-Green fluorescence $\Phi(Na)$ ($S(Na)$ of Fig. 1D). Noting that the calculated $\Phi(Na)$, corresponds to the measured $\bar{F}$, then $Na = \Phi^{-1}(\bar{F})$ gives the concentration of sodium. The preparation specific calibrated response Na versus $\Phi(Na)$ for the known resting concentration $Na^r = 17.4$ mM (Wallin, 1967) is shown in Fig. 2a (thick solid curve).

3.3. Effect of deviation of Na^r

To determine the error of $Na = \Phi^{-1}(\bar{F})$ induced by the standard error of Na^r, two additional curves are plotted in Fig. 2b and c using $Na^r = 17.4 - 0.4 = 17.0$ mM and $Na^r = 17.4 + 0.4 = 17.8$ mM, resulting in a error. When $\Phi(Na) = 0.5$, the error is 5 mM, which is 10%.

To compare IRM with ARM, the corresponding curve for the IRM (d) was obtained by fitting a cubic spline function to the data points for rfmax(Na) shown in Fig. 1D.

For the $\bar{F} = \Phi(Na)$ values (thick marks on horizontal axis) the corresponding $Na = \Phi^{-1}(Na)$ values are shown as thick marks on the vertical axis and crosses on the curve (a). The thick vertical marks on the curve show the difference in mM between the IRM method, $Na = rfmax^{-1}(F)$ (dotted line) and the ARM (solid line), evaluated as

$$\Delta Na = rfmax^{-1}(\bar{F}) - \Phi^{-1}(\bar{F}).$$

When $\bar{F} = 0.3,\ 0.4,\ 0.5,\ 0.6,\ 0.7,\ 0.8$ the corresponding $Na = \Phi^{-1}(\bar{F})$ values are 28.61, 36.48, 55.10, 82.00, 98.53, 119.37 mM and the respective ΔNa values are 1.21, 5.55, 20.17, 10.42, 10.73, 13.59 mM, which are a bit large when absolute concentrations are of interest. Note that when the maximums of each $F(\lambda, Na)E(\lambda)$ do not occur at λ_0 then the corresponding ΔNa values become 0.75, 4.04, 12.15, 4.51, 4.61, 9.31 mM, which are smaller. Thus the use of Φ^{-1} of the ARM method increases the accuracy of measurement compared to rfmax^{-1} of the worst-case IRM method; a calibrated narrow band filter version of ARM would occur between these extremes (a and d curves). If there is induced tracing error (Fig. 1A), then the resultant error is less for the integral than for the maximums of each curve.

Note that up to this point all of the curves are from Na-Green calibration data, PMT efficiency, or have been calculated.

3.4. Measurement of relative fluorescence in nerve terminal

The one axon innervating all the regions indicated in Fig. 3A and B was stimulated by current pulse trains

with a stair-case increase at frequencies 0, 5, 10, 15, 0 Hz for durations of 1.0, 1.75, 3.75, 3.25, 5.00 s, respectively. Fig. 3C shows the relative fluorescence change with respect to background for each region (reg),

$$\bar{F}(reg) = (F_{stim}(reg) - F_{rest}(reg))/F_{rest}(reg),$$

where $F_{stim}(reg)$ and $F_{rest}(reg)$ are the measured fluorescence during stimulation and rest in each region, respectively. The resultant concentration is with respect to rest, which is assumed to be equal in all four regions. Application of the method assumes that $\Phi(Na)$ corresponds to $\bar{F}(reg)$ from measurements,

$$\Phi(Na) \equiv \bar{F}(reg),$$

thus the inverse function Φ^{-1} gives Na,

$$Na = \Phi^{-1}(\bar{F}(reg)).$$

Fig. 4A shows the resulting $\bar{F}(reg)$ on the left axis and Na on the right. Note in Fig. 4A, that the unequal spacing on the Na axis is due to the non-linearity of the $\Phi(Na)$ function.

Fig. 4B shows measured $Na = \Phi^{-1}(\bar{F}(reg))$ versus time for the four regions. Note the change in shape from Figs. 3C, 4A to B, which is due to the non-linearity of the transformations and the $\Phi(Na)$ versus Na curve in Fig. 2. See Table 1 for actual values. The standard errors from the measurements are also converted and hence are not all equal for the initial resting state.

3.5. Net Na+ flux density

The sodium concentration in an axonal varicosity depends on influx due to APs and Na:Ca exchange and removal by the Na:K pump. Does the net Na+-flux density stay constant for increasing stimulus frequency and for the different terminals? To answer this, the net flux density per region per stimulus interval is given by,

$$FD_{reg} = \Delta Na_{reg} V_{reg}/A_{reg} \Delta t,$$

where ΔNa_{reg}, V_{reg}, A_{reg}, and Δt are, respectively $[Na^+]_i$ per region after a stimulus interval minus $[Na^+]_i$ at start of interval, volume of the region, surface area of the region, and duration of the stimulus interval. We approximated the axonal terminals as ellipsoids of revolution with length (len) and diameter (diam). An ellipsoid (prolate spheroid) with major and minor radii $a = \frac{1}{2}$len and $b = \frac{1}{2}$diam, respectively has volume

$$V_{reg} = \frac{4}{3}\pi ab^2,$$

and surface area (Beyer, 1991),

$$A_{reg} = 2\pi\left[b^2 + \frac{a^2b}{c}\sin^{-1}\left(\frac{c}{a}\right)\right],$$

where $c^2 = a^2 + b^2$ and $a > b$. The measurements of the terminals, rank ordered by size are shown in Table 2. Also shown is the area/volume ratio (μm) and its dimensionless normalization as area × r/vol, where $r = \frac{1}{2}$diam.

The resulting flux density is shown in Table 3A. This is better expressed in Table 3B as net FD_{reg} per AP, calculated from Table 3A by dividing by the number of APs during the interval. Except for the large varicosity (# 1) the flux density per AP is approximately the same, which suggests that the sodium channel density is similar per recorded region.

For each stimulus frequency note that FD_{reg}/AP tends to decrease as terminal size increases. As pulse frequency increases, FD_{reg}/AP tends to decrease. This is possibly due to increasing $[Na^+]_i$, which decreases the net Na-driving force, thus reducing Na+ entry. The fact that calculated FD_{reg}/AP is not strictly monotonic decreasing for increasing stimulus frequency and time may be due to either: (1) errors in our estimates of effective terminal shape; (2) non-varicosity axon included; (3) the volume occupied by intracellular organelles such as mitochondria and vesicles; or (4) the effect of a strong dynamic regulatory mechanism controlling $[Na^+]_i$ which compensates for surface area to volume ratio size (see Section 4).

4. Discussion

This study demonstrates how to transform raw calibration curves of emitted fluorescence versus wavelength for different ionic concentrations to: (1) a curve for relative fluorescence versus concentration; then to
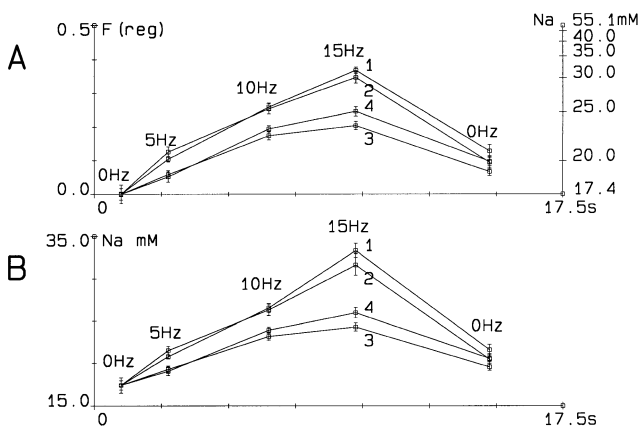

Fig. 4. Sodium response using ARM. (A) Plot of rescaled fluorescence and measured Na in the four regions. The measured signal is resealed to $\bar{F}(reg) = (F(Na(reg)) - F(Na^r))/F(Na^r)$, which assumes for all regions at rest, that $Na = Na^r$. Left vertical axis: $\bar{F}(reg)$. Right vertical axis: $Na = \Phi^{-1}(\bar{F})$. The unequal spacing on the Na axis is due to the non-linearity of the $\Phi(Na)$ versus Na function. (B) Plot of measured Na versus time for the four regions using the ARM method. The signal is $Na = \Phi^{-1}(\bar{F}(reg))$. Note change in shape from Figs. 3C and 4A. Scales: vertical: [15.0, 35.0] mM, horizontal: [0, 17.5] s.

Table 1
Sodium concentration $\bar{x} \pm \sigma_x$ (mM) per region (reg)

Reg #	Stimulus				
	0 Hz, 1.00 s	5 Hz, 1.75 s	10 Hz, 3.75 s	15 Hz, 3.25 s	0 Hz, 5.00 s
1	17.40 ± 0.14	20.77 ± 0.25	26.54 ± 0.38	33.31 ± 0.31	21.56 ± 0.63
2	17.40 ± 0.88	21.48 ± 0.49	26.30 ± 0.50	31.60 ± 0.54	20.45 ± 0.64
3	17.40 ± 0.22	19.27 ± 0.38	23.15 ± 0.40	24.25 ± 0.40	19.54 ± 0.39
4	17.40 ± 0.54	19.04 ± 0.49	23.89 ± 0.31	25.96 ± 0.46	20.54 ± 0.42

(2) relative concentration versus fluorescence; then to (3) concentration versus fluorescence. The givens are the manufacturer's concentration curves for the correct indicator dye batch used, the quantum efficiency of the PMT used, the optical filters used, and the measured relative fluorescence. We applied this method to changes in intracellular concentration based on the Na^+-dependent signal from fluorescence of Na-Green. The computational errors are negligible compared to the possible errors of the measurements of the emission spectra and quantal efficiency of the PMT. Because the standard errors of the emission spectra are not directly available, they were taken as zero to clarify the resulting errors induced by the filters and the computations. With this perspective, the possible sources of error are discussed below.

4.1. Sources of error

1) Because this is a computational procedure, an error in the emission spectra calibration curves will propagate through the procedure and produce an error in the result. To address this issue, calibration curves with mean and standard error of emitted fluorescence from multiple measurements from the same dye sample and from multiple samples could be measured by the experimenter or supplied by the manufacturer (e.g. an ASCII file from a web site). An increase in the number of concentration steps would increase the measurement precision. When standard errors are available, the well known analysis of error can be applied to the calculations to obtain a net error.

2) The resulting calculated curves of Figs. 1D and 2 show small inflection points, not as expected from a simple binding reaction. This is seen in Fig. 2 for

Na > 36 mM, where the linear interpolant function (dashed line) is compared with the cubic spline interpolant (solid line). The measured fluorescence values used yield Na < 33.5 mM, which is less than the 36 mM for any possible measurement error. This inflection is well known for cubic spline interpolants and is the result of less than an optimal number of data points, i.e. the fluorescence versus λ per Na curves from which to compute the cubic spline functions. This would give more abscissa concentration values in Fig. 1D, which originate from the Na^+ concentration curves in Eq. (1)A. For this curve, $Na = \Phi^{-1}(\bar{F})$, we could have used a cubic spline under tension, but this would have added additional complexity, when more data points is the preferred approach.

3) The fluorescence signal is attenuated by passing through tissue. The signal $\bar{F}$ compensates for this (as discussed in Section 2.1). The measurement signal $\bar{F}(\text{reg})$ here is physically the same and directly corresponds with the measurement signal, $\Phi(\text{reg})$. Once the dye and PMT have been calibrated without regard to tissue absorbance, the set-up for this method is then completed by the indicated calculations.

4) The calibrated quantum efficiency curve for each model of PMT must be used because there can be differences between different models. Also the calibration curve for each individual model of PMT must be used because there can be individual differences, although small, between PMTs of the same manufacturer's model. In practice the calibration should not change except with long use. We used the manufacturer's quantum efficiency curve supplied with a new PMT for the measurements.

Table 2
Surface area to volume ratios per region (reg)

Reg #	Len (µm)	Diam (µm)	Area (µm²)	Vol (µm³)	Area/vol (µm⁻¹)	Area × r/vol (l)
2	3.3	1.7	14.9	4.8	3.08	5.13
3	5.0	3.3	47.0	29.1	1.62	4.04
4	8.3	3.3	72.6	48.5	1.50	6.24
1	10.0	6.7	188.0	232.7	0.81	4.04

Table 3
(A) Net Na$^+$ flux density (positive inward) [fmol/μm^2 s]; (B) net Na$^+$ flux density per AP [fmol/μm^2 s AP]; (C) net Na$^+$ flux density after the 95 APs in the 5, 10, 15 Hz stimuli

Reg #	0 Hz	5 Hz	10 Hz		15 Hz	0 Hz[a]
A						
2	0.000	0.758	0.418		0.530	−0.725
3	0.000	0.661	0.640		0.209	−0.583
4	0.000	0.625	0.863		0.425	−0.723
1	0.000	2.384	1.905		2.579	−2.909
B						
2	·	0.087	0.011		0.011	·
3	·	0.076	0.017		0.004	·
4	·	0.071	0.023		0.009	·
1	·	0.272	0.051		0.053	·
C						
	Na (mM)	ΔNa (mM)	Flux density (pmol/(cm^2 AP))			
2	31.60	14.20	0.049			
3	24.25	6.85	0.045			
4	25.96	8.56	0.060			
1	33.31	15.91	0.207			

[a] · indicates efflux.

5) The bandwidth of the detected light passed by the optical filter(s) used affects the accuracy of the measured result. For a standard error of zero in the emission spectral curves (as we used), the ARM approach, which uses fluorescence at all passed wavelengths, is better than the narrow band ARM, which is better than the single wavelength ARM (IRM), where the wavelength is for fluorescence maximum. Noting that the IRM is not used in practice, the difference in the three methods demonstrates that the widest possible wavelength interval gives the most accuracy. Note that the narrow band ARM has a calibration curve which is between the worst-case single wavelength version and the ARM approach.

6) The method requires resting concentration of sodium in the measured region and conversion of S(Na) to Φ(Na), which compensates for signal attenuation in the tissue between source and PMT and corresponds directly to the measured signal. Note the difference in Figs. 3C and 4B for the initial measurements at 0 Hz. In Fig. 3C, F_{rest} is the fluorescence signal per region at 0 Hz. In Fig. 4B, F_{rest} is the fluorescence signal from Na^r. The latter case assumes constant Na^r for all regions in the axon and benefits from the small standard error, 0.4 mM.

4.2. Calibration standards

An analysis of error from error tolerances of the fluorescence emission and PMT quantum efficiency curves or tracing error can be applied to the calculations that yield the calibration curve. Because ratios are used, this source of error would be expected to be much smaller than other sources of error. The increase in accuracy of ionic concentration measurements using the ARM method is practical because it provides an increase in precision of ionic concentration measurements. However, analysis of error, not normally done in biological calibrations, would be welcome once errors of the measured emission spectral curves are available.

4.3. Non-linearities

Regardless of the filter interval used with the ARM method, the curves shown in Fig. 1D or Fig. 2 clearly demonstrate that Na is non-linear with respect to $\bar{F}$. The effects of this non-linearity are further seen in the change in shape of the plot for relative fluorescence versus time (Fig. 3A) and the plot for Na versus time (Fig. 3B).

In a wider context, when a confocal fluorescent measurement system is calibrated using cuvettes of different sodium concentrations and fixed Na-Green concentration, many small increments of sodium concentration must be used to capture the variable slope seen in the plot of Na versus Φ(Na). This reflects the increasing saturation or the dye with sodium. See Figs. 1D and 2.

4.4. Relation of ARM to the F_{max} equation

In the function $F = A_{f}C_{f} + A_{b}C_{b}$, the coefficients are assumed to be for one wavelength, λ, and the equation $F = K_{d}(F − F_{min})/(F_{max} − F)$ is derived. The values of

F_{min} and F_{max} are measured with the filters in place. Since filters pass more than a single wavelength, the equation when $a < \lambda < b$ should be,

$$F = \int_a^b [A_f(\lambda)C_f + A_b(\lambda)C_b]\,d\lambda.$$

The measured F_{max}, F_{min} method is similar to the ARM, but uses a different calibration curve. Further, the usual practice of measuring F_{max} is to have all of the indicator dye bound; that is, to increase concentration of the target ion to ∞, by lysing the cell with an ionophore and titrating the ion. For the case of calcium where the usual intracellular concentration is close to zero this is practical. In contrast, when the resting concentration is high as in the case of Na^+, the approach of ARM is possibly more accurate. At least the preparation destructive measurement of F_{max} is not required.

4.5. Sodium increase

We demonstrated that $[Na^+]_i$ increases monotonically by twofold for the frequency steps of 5, 10, 15 Hz over 8.75 s. This measurement of an increase during low frequency pulse trains correlates with the indirect demonstration of the effects of sodium accumulation (which was not measured) during a longer duration (7 min) at higher frequency (33 Hz) reported by Mulkey and Zucker (1992).

4.6. Buffering

The standardization curves were obtained using the indicator in a different buffer solution than those within the experimental preparation. Different buffering environments can result in differences of emission signals. Since this is difficult to control and we do not know the full extent of the buffering abilities within the crayfish motoneuron cytoplasm, this is a moot point; but the reader should be aware of the issue.

4.7. Surface to volume ratio

The twofold increase of $[Na^+]_i$ for 15 Hz stimulation is in contrast to measurements in *Sepia* giant axon (Hodgkin and Keynes, 1955), where stimulation at 156 Hz for 4 min at 18 °C causes a rise in $[Na^+]_i$ from 40 to 72 mM, an 0.8-fold increase, which is substantially less for many more stimulus APs over a longer time. This is due to the different internal and external concentrations of Na^+ and K^+ in squid versus crayfish and possibly different Na:K pumping rates. Also a larger surface area to volume ratio, (σ) in crayfish nmj terminals compared with squid giant axon, plays a role. In general, a larger σ, means that as ionic flux density increases, the ionic concentration increases faster than for a smaller σ. Also, there possibly could be different rates of pumping and differential loss due to the surface area-to-volume relationship.

For a circular cylinder of radius, r, and length, L, with circumference, C, and cross-sectional area, A, the area-to-volume ratio is,

$$\sigma = \frac{CL}{AL} = \frac{2\pi r L}{\pi r^2 L} = \frac{2}{r}.$$

For a crayfish varicosity of diameter 4 μm, $\sigma = 1/\mu m$.

A squid giant axon in cross-section is an ellipse with major and minor diameters 400 and 200 μm, respectively. An ellipse with major and minor radii, a and b, respectively, with eccentricity $k = [(a^2 - b^2)/b^2]^{1/2}$, has area $A = \pi ab$ and circumference (Rade and Westergren, 1995),

$$C = 4a \int_0^{(1/2)\pi} [1 - k^2 \sin^2 \theta]^{1/2}\,d\theta,$$

which integrated numerically gives $\sigma = 7.7 \times 10^{-3}/\mu m$. Since σ for crayfish axon terminal is 7700 times larger than for squid, in crayfish Na^+ influx has a much larger influence on $[Na^+]_i$ than in squid. Note that σr for a circular cylinder is constant and an elliptical cylinder is near constant.

When the net ΔNa for the 95 APs in the 5, 10, 15 Hz stimuli intervals is converted to pmol/(cm^2 AP) (Table 3C) the values for each region are 1–10% of the value 5 pmol/(cm^2 AP) in response to 156 Hz stimulation for 4.0 min (37 440 APs) reported by Hodgkin and Keynes (1955) (Table 3) in *Sepia* giant axon for net influx and efflux. Assuming that entry of $[Na^+]_i$ per channel is the same for both axon preparations, this suggests that the Na^+ channels/cm^2 in the crayfish nmj terminal are 1–10% of the density in *Sepia* giant axon. This suggests that there is regulation of the density of Na^+ channels to cope with the large surface area to volume ratio.

We demonstrated: (1) how to transform measured emitted fluorescence versus ionic concentration curves to a calibration curve of concentration versus fluorescence; (2) the sources of error in using this calibration method; (3) the use of the ARM to show the effects of optical filter bandwidth on accuracy; (4) how to calculate the calibration signal when using representative optical filters; (5) a correspondence of the calibration curve to the K_d, F_{max}, F_{min}, concentration equation; (5) a method of ionic concentration measurement which does not require determination of F_{max}, usually by application of a preparation destructive ionophore; (7) application of the ARM to measure sodium ion concentration in crayfish nmj; (8) an increasing saturation of $[Na^+]_i$ during increasing pulse train frequencies at low physiological stimulus frequencies; (9) the analy-

sis of surface area to volume ratio in interpreting ionic flux density; and (10) the Na^+ channel density in small axon presynaptic terminals is 1–10% of that in *Sepia* giant axon.

It would useful on the same preparation to directly compare our method with the method for ratio-metric Na^+ indicator dye SBFI (Diarra et al., 2001). Two types of dyes have been used for Ca^{2+} (Suzuki et al., 2000). The variation of $[Na^+]_i$ at rest in different regions of small axons (Table 1) and different net flux-densities per AP (Table 3) need to be further investigated.

In conclusion, we have shown that: (1) published calibration curves can provide some quantitative estimates of ion concentration; (2) the bandwidth of the emission filters can affect the dynamic range of the indicator; and (3) $[Na^+]_i$ can increase in an axon during a pulse train. We have extended the usefulness of near monochromatic fluorescent indicator dyes with the confocal microscope for physiological experiments.

Acknowledgements

References

Atwood HL. Membrane physiology of crustacean neurons. In: Podesta RB, editor. Membrane Physiology of Invertebrates. New York: Marcel Dekker, Inc, 1982:341–407.

Beyer WH. Standard Mathematical Tables and Formulae, 29th ed. Bocca Raton, FL: CRC Press, 1991:112.

Cooper RL, Winslow JL, Govind CK, Atwood HL. Synaptic structural complexity as a factor enhancing probability of calcium-mediated transmitter release. J Neurophysiol 1996;75(6):2451–66.

Diarra A, Sheldon C, Church J. In situ calibration and $[H^+]$ sensitivity of the fluorescent Na^+ indicator SBFI. Am J Physiol Cell Physiol 2001;280:C1623–33.

Grynkiewicz G, Poenie M, Tsien RY. A new generation of Ca^{2+} indicators with greatly improved fluorescence properties. J Biol Chem 1985;260(6):3440–50.

Harootunian AT, Kao JPY, Eckert BK, Tsien RY. Fluorescence ratio imaging of cytosolic free Na^+ in individual fibroblasts and lymphocytes. J Biol Chem 1989;264(32):19458–67.

Hodgkin AL, Keynes RD. Active transport of cations in giant axons from *Sepia* and *Loligo*. J Physiol 1955;128:28–60.

Horton HR, Moran LA, Ochs RS, Rawn JD, Scrimgeour KG. Principles of Biochemistry, 2nd ed. Upper Saddle River, NJ: Prentice-Hall, 1996.

Johnson LW, Riess RD. Numerical Analysis. Reading, MA: Addison-Wesley, 1977:200–9.

Minta A, Tsien RY. Fluorescent indicators for cytosolic sodium. J Biol Chem 1989;264(32):19449–57.

Molecular Probes Handbook. Fig. 24.5, bottom, 1998.

Mulkey RM, Zucker RS. Posttetanic potentiation at the crayfish neuromuscular junction is dependent on both intracellular calcium and sodium ion accumulation. J Neurosci 1992;12(11):4327–36.

Press WH, Flannery BP, Teukolsky SA, Vetterling WT. Numerical Recipes in C. New York: Cambridge University Press, 1988:94–8.

Rade L, Westergren B. Mathematics Handbook for Science and Engineering. Lund, Sweden & Cambridge, MA: Birkhauser, 1995:81.

Regehr WG. Interplay between sodium and calcium dynamics in granule cell presynaptic terminals. Biophys J 1997;73(5):2476–88.

Suzuki S, Osanai M, Murase M, Suzuki N, Ito K, Shirasaki T, Narita K, Ohnuma K, Kuba K, Kijima H. Ca^{2+} dynamics at the frog motor nerve terminal. Pflugers Arch Eur J Physiol 2000;440:351–65.

Szmacinski H, Lakowicz JR. Sodium green as a potential probe for intracellular sodium imaging based on fluorescence lifetime. Anal Biochem 1997;250(2):131–8.

Tsien RY, Waggoner A. Fluorophores for confocal microscopy. In: Handbook of Biological Confocal Microscopy, 2nd ed. New York: Plenum Press, 1995:267–79.

Tucker T, Fettiplace R. Confocal imaging of calcium microdomains and calcium extrusion in turtle hair cells. Neuron 1995;15:1323–35.

Wallin BG. Intracellular ion concentrations in single crayfish axons. Acta Physiol Scand 1967;70:419–30.

Winslow JL, Bjerknes M, Cheng H. Three-dimensional reconstruction of biological objects using a graphics engine. Comp Biomed Res 1987;20:583–602.

Winslow JL, Cooper RL, Atwood HL. Accounting of Ca^{2+} and Na^{2+} in presynaptic axon varicosities. Abst Soc Neurosci 1996;22:494.12.

Wojtowicz JM, Atwood HL. Correlation of presynaptic and postsynaptic events during establishment of long-term facilitation at crayfish neuromuscular junction. J Neurophysiol 1985;54(2):220–30.